2006

Gene Expression and Discovery During Lens Regeneration in Mouse: Regulation of Epithelial to Mesenchymal Transition and Lens Differentiation

Mario Medvedovic

Craig R. Tomlinson

Mindy Kay Call

Matthew Grogg

Panagiotis A. Tsonis
University of Dayton, ptsonis1@udayton.edu

Molecular Vision 2006; 12:422-40 <http://www.molvis.org/molvis/v12/a49/>
Received 29 November 2005 | Accepted 18 April 2006 | Published 8 May 2006

Gene expression and discovery during lens regeneration in mouse: regulation of epithelial to mesenchymal transition and lens differentiation

Mario Medvedovic,[1] Craig R. Tomlinson,[1] Mindy K. Call,[2] Matthew Grogg,[2] Panagiotis A. Tsonis[2]

[1]Genomics and Microarray Laboratory, Department of Environmental Health, Center for Environmental Genetics, University of Cincinnati Medical School, Cincinnati, OH; [2]Laboratory of Molecular Biology, Department of Biology, University of Dayton, Dayton, OH

Purpose: It has been shown that after extracapsular lens removal by anterior capsulotomy in the mouse, the lens can be regenerated. However, as the capsular bag is filled with fibers, epithelial to mesenchymal transition (EMT), an event which is common after cataract surgery as well, takes place during early stages. This study, using a unique mouse model, was undertaken to identify novel regulators and networks in order to more clearly understand secondary cataracts at the molecular level.

Methods: We examined global gene expression via microarray analysis of mouse lens regeneration after extracapsular surgery. Gene expression at different times after surgery was correlated with the processes of EMT, which is seen in the initial stages of regeneration, and lens fiber differentiation, which occurs later.

Results: Several notable patterns were observed from the gene clustering data. It was obvious from the analysis that initially there is a response to injury, extensive matrix remodeling, and severe downregulation of genes encoding lens structural proteins. The patterns returned gradually to normal three weeks after surgery. New genes were identified from the clustering results that might be potential regulators of EMT and lens differentiation.

Conclusions: With this approach, we demonstrated the utility of a mouse model to study secondary cataracts at the molecular level. Extension of these studies in mice with known mutations affecting EMT or lens differentiation should allow the identification of the crucial molecular players that could lead to better treatments of secondary cataracts.

Traditionally, the newt has been hailed as the most powerful animal model for lens regeneration [1,2]. True enough, adult newts always replace their lens following removal. Lens regeneration in newts is achieved by transdifferentiation of the pigment epithelial cells from the dorsal iris. Other amphibia, such as frogs, are capable of lens regeneration by transdifferentiation of the cornea, but only during a short window of time before metamorphosis [3]. The situation in higher vertebrates, especially in mammals, is very different. Lens regeneration has been shown in rabbits, but only if the lens capsule is left behind [4]. Obviously, some lens epithelial cells remain attached to the lens capsule and they differentiate to lens fibers to "regenerate" a lens, which nevertheless is not perfect. Some similar, but limited, observations have been seen in cats [5]. The studies with rabbits suggest that while lens regeneration does not follow the same traditional road of transdifferentiation as in newts, regeneration can nevertheless occur by differentiation of lens epithelial cells remaining on the capsule. Rabbits (or cats), however, are not favorable mammalian animal models for approaching the problem of lens regeneration with the frontline technology of molecular biology and, therefore, extensive studies at the molecular level are hindered. We reported previously that when the lens is removed in adult mice, leaving the capsule in the eye cavity, lens fibers rapidly differentiate from the adherent lens epithelial cells and fill the capsule within a few weeks, and is not limited to Soemmerring's ring only [6]. Such "regeneration" of the lens is quite remarkable and has been reported in mouse and rats by others as well [7,8]. Importantly, epithelial to mesenchymal transition (EMT) has been observed at the initial stages in mice undergoing regeneration, indicating that the process undergoes an initial phase of repair and of lens differentiation.

EMT is a prominent process after cataract surgery. During modern cataract surgery, extracapsular lens removal allows the synthetic lens to be placed on the remaining capsule. However, adherent lens epithelial cells (LECs) still persist in most cases. LECs tend to transdifferentiate to mesenchymal cells, and this process leads to the so-called posterior capsule opacification (PCO), which requires expensive laser treatment, even though such procedures have been considerably reduced recently because of the state of the art instruments and the techniques applied [9]. The most common experimental procedures to study EMT in LECs are either treating LECs in vitro or to injure lenses in vivo. Both rats and mice are commonly used for this assay. The in vivo procedure is usually performed by injury of the anterior subcapsular region with a needle. Such injury leads to cataract-related changes involv-

Correspondence to: Panagiotis A. Tsonis, Laboratory of Molecular Biology, Department of Biology, University of Dayton, Dayton, OH, 45469-2320; Phone: (937) 229-2579; FAX: (937) 229-2021; email: panagiotis.tsonis@notes.udayton.edu

ing EMT. Culture of capsular bags from humans is another experimental system where proliferation and transdifferentiation of LECs can be studied [10]. In these experiments, the capsular bags from deceased donors can be placed in culture, and the degree and development of EMT can be assessed in vitro. Such studies have provided important information about the factors involved, but are limited for genetic manipulations. TGF-β is considered an important factor in the initiation of EMT [11-13].

The ability of mice to regenerate the lens under the outlined conditions provides us with a valuable animal model system to study basic biology of EMT at the molecular level and to identify targets that eventually could lead to further understanding of the medical complications and the design of effective treatments. The availability of mutant mice and microarray analysis enables us to profile genomic activity during EMT, which is otherwise impossible to carry out. Furthermore, such studies as the ones presented here might elucidate factors that will improve the quality of the regenerated lens, information that will be important in future applications when the lens is accidentally damaged. In the present study, we have examined gene expression during different stages of lens regeneration in mice via microarray hybridization and analysis. Our results provide unique and interesting insights in gene regulation during EMT and lens differentiation.

METHODS

Surgical procedures: C57BL mice (six to eight months old) were anesthetized with either intraperitoneal or subcutaneous injections of ketamine (87 mg/kg) and xylazine (13 mg/kg). Mice were also subcutaneously given the analgesic buprenorphine (2 mg/kg) preemptively. Pupils were dilated with the use of 1% tropicamide and 2.5% phenylephrine hydrochloride. A corneal incision was made, and anterior capsulotomy was performed. The lens was then removed by pushing the eye cavity with forceps. The anterior chamber was filled with sodium hyaluronate. In our hands, this procedure effectively removes the whole lens (we have examined removed lenses and lentectomized eyes by histology) and leaves the capsule behind, eventually with LECs. Figure 1 shows the morphology of the capsule one day after lens removal.

Experimental design: Microarray hybridization methods were used to obtain global gene expression profiles from intact and regenerating eyes after extracapsular lens removal in C57BL mice eight weeks of age. We examined four times, time 0 at the time of lens removal and 1, 2, and 3 weeks after surgery. In our previous publication [6] we presented a histological study of the early stages of these events. During week one we observed fiber differentiation and EMT. Week two was basically marked by increased fiber differentiation and a lower degree of EMT. By week three, EMT was virtually absent. Since the goal of this study was to identify genes that affect EMT and lens fiber differentiation, these times were sufficient because both EMT and fiber differentiation occur rapidly after surgery and follow a particular course.

A 70-mer oligonucleotide library from Operon Technologies, Inc. (Huntsville, AL) representing 24,878 known mouse genes (e.g., genes involved with cell signaling, apoptosis, cell proliferation, etc.; including most, if not all, of the available

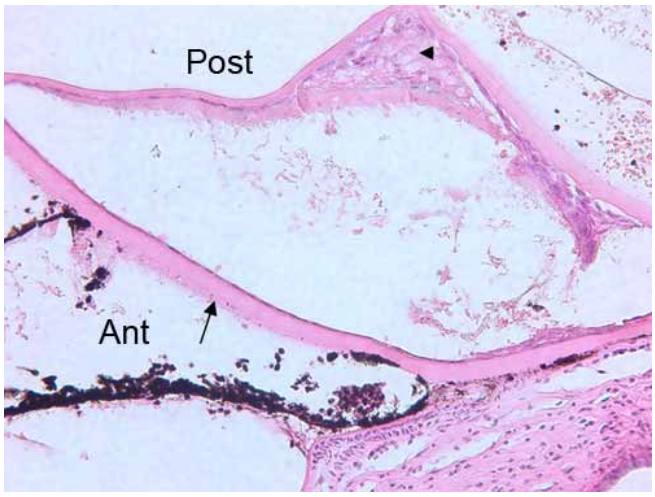

Figure 1. Histological section through a capsular bag one day post-lentectomy. The arrowhead marks where some cells remain at the posterior (Post) area of the capsule. The arrow indicates the anterior (Ant) part of the capsule.

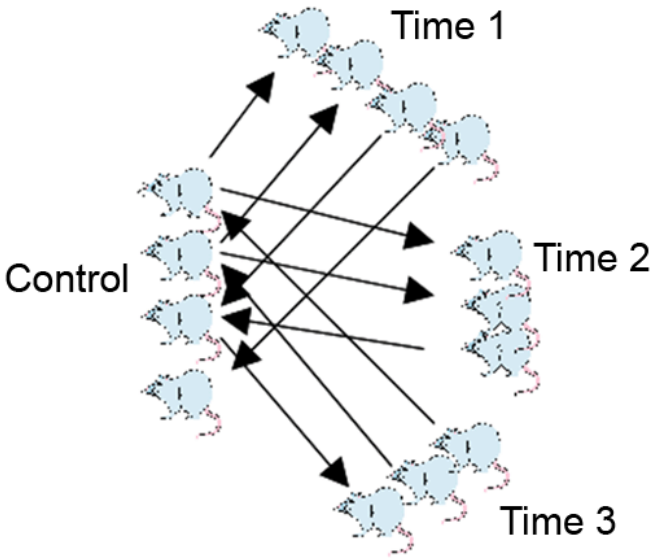

Figure 2. Experimental design for the microarray studies. The indicated time periods of 1, 2, and 3 represent weeks post-lentectomy from time 0 (Control). Each mouse represents a biological replica for a given experimental condition. An arrow denotes a microarray slide comparison between a given pair of mice. Arrows for a given experimental comparison represent "dye flips". Our statistical model does indeed unequivocally factor out the gene-specific dye effect from the estimates of differential expression. This is achieved by fitting a linear statistical model with a "dye" effect, as described in the data normalization and analysis section of the methods, to each gene separately. This approach has been demonstrated to work well in unbalanced situations such as the week 2 and 3 comparisons [35].

known genes involved in regeneration) were used for the microarray experiments.

As depicted in Figure 2, each regenerating tissue was directly compared to the corresponding intact tissue. RNA from control tissues was obtained from four independent animals and hybridized with RNA obtained from the same number of independent animals at week one and three animals at weeks two and three after the surgery. Biological variation was accounted for by including the multiple biological replicates per experimental condition. Our statistical model does indeed unequivocally factor out the gene-specific dye effect from the estimates of differential expression. This is achieved by fitting a linear statistical model with a "dye" effect, as described in the data normalization and analysis section of the methods, to each gene separately. This approach has been demonstrated to work well in unbalanced situations such as the week two and three comparisons.

Isolation of tissues and total RNA: Total RNA was isolated by standard methods using the Nucleospin RNA purification kit from BD Bioscience (San Jose, CA). We analyzed the quality of mRNA using an Agilent Bioanalyzer 2100 and NanoDrop 1000.

Target labeling: For each hybridization experiment (a microarray slide), total RNA from two single animals were used. Approximately 10 μg of total RNA was used for each Cy-3 or Cy-5 labeling procedure. cDNA target was synthesized using an indirect labeling method, in which aminoallyl-dUTP (7:3 ratio of aa-dUTP:TTP) was incorporated in the cDNA via an oligo(dT) primed reaction by reverse transcriptase (Superscript III; Invitrogen, Carlsbad, CA). The cDNA was decorated with Cy-3 and Cy-5 (Cy Dye™ Post-Labeling Reactive Dye Packs; Amersham, GE Healthcare, Piscataway, NJ) following the accompanying instructions. When necessary, the RNA was amplified using the Amino Allyl MessageAmp™ kit from Ambion (Austin, TX), which in our hands produced approximately 50-120 μg of amplified RNA (aRNA) with the incorporated amino allyl nucleotides starting from one μg of total RNA (10 μg of each aRNA was used per slide). The aRNA is an accurate representation of the original total cellular RNA [14].

Microarray hybridization: The mouse 70-mer oligonucleotides were suspended in 3X SSC at 30 μM and printed at 22 °C and 65% relative humidity on aminosilane-coated slides (VSA-25C; Cel Associates, Inc. Pearland, TX) using a high-speed robotic OmniGrid machine (GeneMachines; San Carlos, CA) with Stealth SMP3 pins (Telechem, Sunnyvale, CA) [15,16]. The microarray slides were placed in prehybridization buffer (5X SSC, 0.1% SDS, and 1% BSA) and incubated at 48 °C for 45-60 min. The slides were washed twice in deionized water and used immediately for hybridization (2X hybridization buffer: 50% formamide, 10X SSC, and 0.2% SDS). The Cy-3 and Cy-5 labeled targets were suspended in nine μl water and heated at 95 °C for 3 min. The following were added to each tube of labeled target to inhibit nonspecific hybridization: eight μl of 1 mg/ml COT1-DNA (Roche Diagnostics, Basel, Switzerland), two μl of 10 mg/ml poly(A)-DNA (Sigma, St. Louis, MO), and two μl of 4 mg/ml yeast tRNA (Sigma).

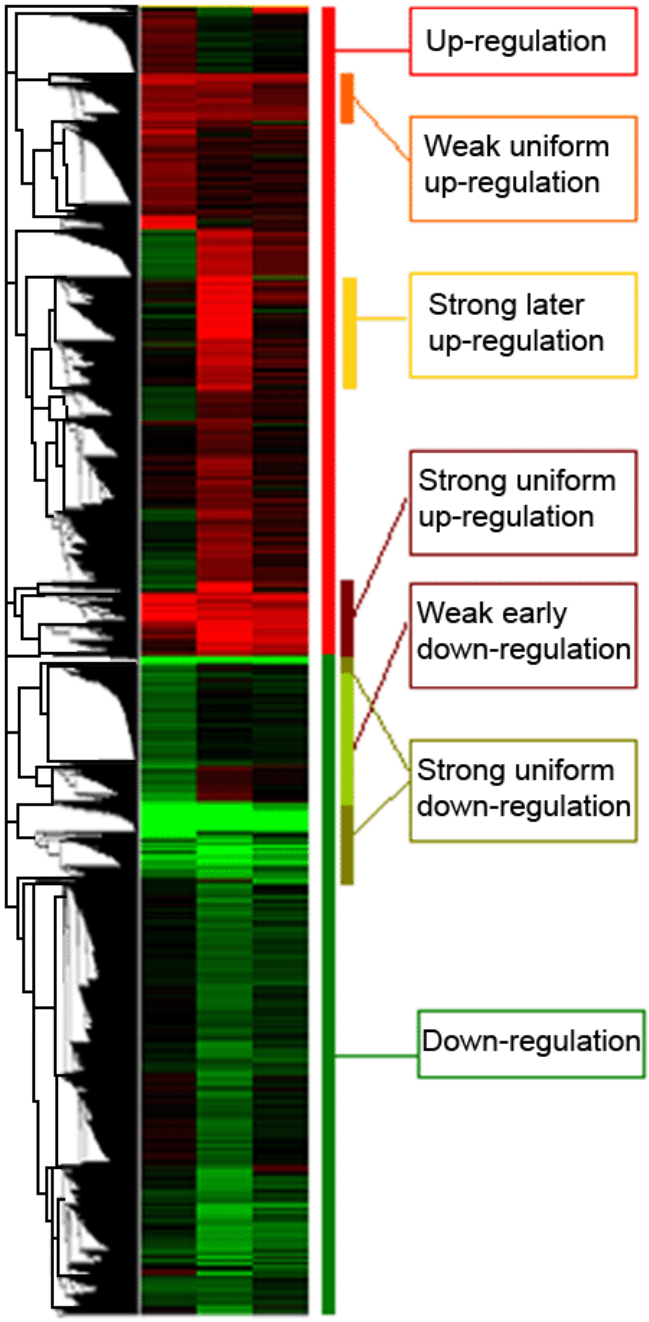

Figure 3. Heat map from the cluster analysis of 2,094 differentially expressed genes. The hierarchical clustering of all genes with each line representing expression levels for a gene as compared to control and each column a time (1, 2, and 3 weeks post-lentectomy). Shades of red indicate increased expression and the shades of green decrease. Genes are grouped according to a particular expression pattern (i.e., upregulation or downregulation) and within these two groups in other sub-groups, such as strong uniform upregulation, strong uniform downregulation, etc. Five clusters of co-expressed genes outlined in the figure were statistically significantly enriched for genes in at least one GO category.

Next, 21 µl of 2X hybridization buffer preheated to 48 °C was added to the target mixture, mixed well, and centrifuged. The labeled target was applied to the prehybridized microarray slides, covered with a 22x60 mm glass cover slip, and placed in a sealed hybridization chamber (Corning, Acton, MA). The sealed chamber was placed in a 48 °C water bath and incubated for 40-60 h. For the posthybridization washes, the coverslips were removed in 1X SSC, 0.1% SDS, and 0.1 mM DTT at 48 °C, and the slides were agitated for 15 min. The microarray slides were transferred to a staining dish containing 0.1X SSC, 0.1% SDS, and 0.1 mM DTT at 48 °C and agitated for 5 min. The aforedescribed wash was repeated two more times. The slides were then washed two times in 0.1X SSC and 0.1 mM DTT at room temperature and agitated for 5 min. The slides were then spin dried [17].

Scanning and data generation: Imaging was carried out using a GenePix 4000A and GenePix 4000B (Axon Instruments, Union City, CA) with GenePixPro 5.0 software. Images were captured in JPEG and TIFF files, and the DNA probes were measured by the adaptive circle segmentation method. Information extraction for a given spot was calculated using the median value for the signal pixels minus the median value for the background pixels to produce a gene set data file for all the DNA spots. The Cy-3 and Cy-5 fluorescence signal intensities were normalized by adjusting total fluorescence levels.

Data normalization and analysis: The data representing raw spot intensities generated by GenePix® Pro version 5.0 was analyzed to identify differentially expressed genes. Data normalization was performed in three steps for each microarray separately [17]. First, channel-specific local background intensities were subtracted from the median intensity of each channel (Cy3 and Cy5). Second, background adjusted intensities were log-transformed and the differences (R) and averages (A) of log-transformed values were calculated as $R=\log_2(X1/X2)$ and $A=[\log_2(X1 \quad X2)]/2$, where X1 and X2 denote the Cy5 and Cy3 intensities after subtracting local backgrounds, respectively. Third, data centering was performed by fitting the array-specific local regression model of R as a function of A. The difference between the observed logarithmic ratio and the corresponding fitted value represented the normalized log-transformed gene expression ratio. Normalized log-intensities for the two channels were then calculated by adding half of the normalized ratio to A for the Cy5 channel and subtracting half of the normalized ratio from A for the Cy3 channel. A statistical analysis was performed for each gene separately by fitting the following mixed effects linear model. $Y_{ijk}=\mu+A_i+C_k+T_j+\varepsilon_{ijk}$, where Y_{ijk} corresponds to the normalized log-intensity on the i^{th} array (i=1,...,10), at the j^{th} time (j=1,2,3), and labeled with the k^{th} dye (1 for Cy5 and 2 for Cy3). µ is the overall mean log-intensity, A_i is the effect of the i^{th} array, T_j is the effect of the j^{th} time, and C_k is the effect of the k^{th} dye. Assumptions about model parameters were the same as described in the literature [18] with array effects assumed to be random and treatment and dye effects assumed to be fixed. Statistical significance of differential expression between RNA samples at each time after the treatment, after adjusting for array and dye effects, was assessed by calculating p values and applying False Discovery Rates (FDR) multiple hypotheses testing [19,20]. Data normalization and statistical analyses were performed using SAS statistical software package (SAS Institute Inc., Cary, NC).

Cluster analysis: Clustering was performed with the Bayesian infinite mixture (BIM) model-based clustering for replicated microarray data [21,22] using replicated normalized logarithmic ratios from each microarray. BIM model-based clustering allowed for the fitting of the statistical mixture model without knowing the number of clusters in the data [22]. The statistical model was fitted using the Gibbs sampler, and hierarchical clustering was produced by treating pair-wise posterior probabilities as the similarity measure and applying the traditional average-linkage principle. The clustering results were displayed using the TreeView program [23].

Functional clustering: Clusters of co-expressed gene identified by the cluster analysis were correlated with functional groupings defined by Gene Ontologies (GO) [24]. Clusters of genes with significantly over-represented genes from specific GO categories were identified using the EASE software [25]. Statistical significance of over-representation of genes from a cluster in any given GO category was assessed using the Fisher's exact test with the Benjamini-Hochberg adjustment for multiple hypothesis testing [19]. A GO category was considered to be significantly associated with a cluster if it contained more than one gene from the cluster and the adjusted Fisher's exact p value was less than 0.1.

Quantitative real-time polymerase chain reaction: RNA was isolated from intact eyes and eyes undergoing lens regeneration using Tri Reagent® (Molecular Research Center, Inc., Cincinnati, OH) according to the manufacturer's instructions. RNA (0.75 µg) was used to synthesize cDNA using the iScript™ cDNA Synthesis Kit (BioRad). All Real-Time PCRs were performed using the iCycler™ (BioRad). For each Real-Time PCR reaction run in triplicate, 2 µl of cDNA, 800 nM primers, and iQ™ SYBR® Green Supermix (BioRad) were used. The data were analyzed using the Pfaffl method [26].

RESULTS & DISCUSSION

Labeled target representing mouse mRNA from lens was used to hybridize to arrayed 70-mer probes representing nearly 25,000 mouse genes. Gene expression profiles of regenerating lens (one, two, and three weeks post-lentectomy) were compared to the expression profiles of intact lens (Figure 1). We identified the genes that were significantly differentially expressed during the regeneration process. In all, we identified 2,094 genes that showed regulation during regeneration (FDR<0.05 in at least one comparison). Six clusters of co-expressed genes defining distinct patterns of expression were significantly correlated with at least one GO category (FDR<0.1 and more than one gene from a cluster was a member of a given GO category).

A general pattern emerged indicating that during the first week post-lentectomy, there was an increase in RNA levels of genes involved in tissue repair, inflammation, and reorganization of the cytoskeleton and the extracellular matrix (Figure

TABLE 1.

GenBank accession	Gene name	Average expression	Fold changes Week 1	Week 2	Week 3
J05605	Thrombospondin 1 precursor	45	1.45	15.23	3.24
X81627	Neutrophil gelatinase-associated lipocalin precursor	141	4.26	5.27	6.93
X51547	P lysozyme structural	3781	3.39	6.76	3.43
M33960	Serine (or cysteine) proteinase inhibitor	436	5.49	4.13	3.46
AF071068	Dopa decarboxylase	1379	2.92	6.17	3.16
BC002069	Lysozyme	14018	3.63	5.29	3.12
AK018742	Procollagen, type VIII, alpha 1	481	1.55	7.62	2.75
M26498	Endothelin-2 precursor	1809	5.69	2.26	2.56
AK048616	Similar To Cdna Flj10680	40	1.02	8.41	1.01
BC013651	Serine (or cysteine) proteinase inhibitor, clade A, member 3N	3583	3.96	2.44	3.54
D90343	Tenascin C	351	5.24	2.11	1.93
AK003674	Collagen triple helix repeat containing 1	2832	4.92	2.4	1.8
BC006783	Connective tissue growth factor	3595	2.64	3.9	2.51
U49430	Ceruloplasmin	968	2.32	4.01	2.39
M17243	Tissue inhibitor of metalloproteinase 1	888	3.27	2.62	2.75
AJ223208	Cathepsin S	910	2.59	3.24	2.62
BC030071	Calcitonin/calcitonin-related polypeptide, alpha	128	2.33	2.89	3.05
X97650	Myosin IF	1796	3.37	2.49	2.32
BC016551	Macrophage scavenger receptor 2	330	1.83	3.29	2.83
AF077829	TYRO protein tyrosine kinase binding protein	937	1.88	3.61	2.4
AF213458	Cytochrome P450 4F 18	356	2.54	2.65	2.68
AF213458	Triggering receptor expressed on myeloid cells 2b	745	1.67	3.42	2.75
L04264	Protein-lysine 6-oxidase precursor	3220	4.57	1.69	1.51
AF061272	C-type lectin	303	2.22	3.42	2.08
X58861	Complement component 1, q	1652	1.73	3.56	2.38
X60929	Low affinity Ig gamma Fc region rec. III pre.	398	2.28	3.02	2.34
M73490	Apolipoprotein E	3890	1.63	3.83	2.15
BC027425	Membrane-spanning 4-domains	907	3.53	2.43	1.57
BC021539	Allograft inflammatory factor 1	557	3.01	2.75	1.74
AK010252	Leucine-rich repeat-containing 2	553	2.96	2.27	2.24
U47327	Histocompatibility 2	104	1.15	3.76	2.52
AF175282	Disintegrin-like and metalloprotease with thrombospondin	431	2.65	2.69	1.93
U05264	Glycoprotein 49 B	1722	2.31	2.55	2.37
AF290914	Stabilin 1	547	2.68	2.85	1.69
X92959	Complement C1Q subcomponent	3207	2.24	2.76	2.2
D13664	Osteoblast specific factor 2	1752	3.61	1.87	1.71
X93035	Chitinase 3-like 1	6450	1.89	3	2.27
AK004165	Regulator of G-protein signaling 5	148	1.66	3.79	1.69
U42327	Vascular cell adhesion protein 1 precursor	1972	2.63	2.02	2.44
M18524	H-2 class I histocompatibility antigen	328	1.43	3.16	2.47
AK018713	Cytochrome b-245	699	1.57	2.9	2.57
M69069	Histocompatibility 2, D region locus 1	301	1.11	3.63	2.28
AK014036	Brca1 interacting protein	48	1.11	4.31	1.54
M64866	Thrombospondin 2	2412	3.79	1.34	1.75
AK033376	Similar to Acetyl-Coa Synthetase	114	1.41	3.61	1.84
Y11758	Biglycan	3736	2.19	2.28	2.35
U83172	Paired-Ig-like receptor B	1662	3.35	2.16	1.28
AF063937	Serine (or cysteine) proteinase inhibitor, CLADE B	371	4.35	1.39	1.04
L33416	Extracellular matrix protein 1	11967	2.74	2.07	1.96
X92960	Complement C1Q subcomponent, C chain precursor	3030	2.22	2.27	2.19
AF053757	C3A anaphylatoxin chemotactic receptor	272	2.93	2.49	1.20

Top 50 genes with the greatest increase in relative mRNA expression levels of regenerating lens compared to intact control lens 1, 2, and 3 weeks post-extracapsular surgery. For a better visual presentation of the regulated genes at 1, 2, and 3 weeks, the times that each gene is highest is marked in red.

3). On the other hand, there was a significant decrease in RNA levels of genes encoding lens structural proteins, such as crystallins and other lens-fiber specific markers. As differentiation and growth of the lens ensued, some of the differentially expressed genes gradually returned to control levels of expression. The profile of the crystallins indicated that their synthesis followed the normal developmental program. At the same time, we observed that some genes never reached control levels. Another interesting and novel discovery from the clustering analysis was that RNA levels decreased for genes

Table 2.

GenBank accession	Gene name	Average expression	Fold changes		
			Week 1	Week 2	Week 3
BC021649	cAMP responsive element binding protein 1	6892	-13.62	-18.28	-13.79
NM_153601	Glutamate-ammonia ligase	19389	-17.18	-15.45	-11.07
NM_178922	Hypermethylated in cancer 2 protein	317	-7.66	-14.77	-8.49
AF104312	Hydroxyacid oxidase 1, liver	129	-3.94	-14.38	-11.74
S83259	Homeobox protein NKX-2.2	1773	-9.73	-10.93	-8.02
BC004700	Kruppel-like factor 7	12179	-10.64	-10.48	-4.57
Y13606	Beaded filament structural protein in lens-CP94	6252	-7.96	-9.24	-7.53
S81982	Nitric-oxide synthase, brain	1606	-7.95	-8.12	-4.76
M64544	Crystallin, gamma C	4184	-15.98	-1.72	-2.21
AF349659	Thioredoxin reductase 3	1971	-7	-6.86	-5.46
AF047542	Cytochrome P450	13609	-4.26	-10.12	-3.32
U21110	Signal transducer and activator of transcription 5B	5124	-10.98	-4.58	-1.7
AJ304860	Phakinin	868	-5.49	-5.83	-3.85
AF309072	Lactase-like	1556	-4.41	-6.68	-3.57
BC025817	FAD-synthetase	13552	-6.18	-4.78	-3.57
AJ272229	Crystallin, beta B3	13126	-4.46	-6.07	-3.67
AF277385	Prostatic steroid binding protein C1	204	-1.11	-11.03	-1.97
AF320075	Lens fiber membrane intrinsic protein	1709	-4.89	-5.21	-3.65
AJ239052	Crystallin, beta A1	31909	-2.24	-8.16	-2.85
NM_172635	Expressed sequence AV312086	543	-3.68	-5.65	-3.85
AF072881	WD-40-repeat-containing protein	930	-2.31	-5.98	-4.84
AK053869	Crystallin, beta B1	13272	-4.78	-4.99	-3.05
U36576	Nuclear factor of activated T-cells	1711	-3.39	-5.66	-3.73
U08095	Keratin, type cytoskeletal 12	27443	-8.61	-2.43	-1.69
AK031386	Molecule interacting with Rab13	69	1.16	-9.99	-3.74
AF334607	Dnase2-like acid Dnase	289	-3.9	-6.36	-2.26
AJ224342	Gamma crystallin D	33050	-7.29	-3.29	-1.61
Z22573	Gamma crystallin B	36961	-8.33	-1.53	-2.06
AK003904	Ars component B	13252	-6.75	-3	-1.41
AB037890	Splicing factor 3b	2464	-4.46	-3.59	-2.54
U03562	Heat shock protein 1	11548	-4.09	-2.97	-3.2
AF099938	Complement component C1Q	901	-3.38	-2.72	-3.83
AF000143	Lens fiber major intrinsic protein	2291	-2.93	-4.93	-1.76
BC032251	Brain-specific angiogenesis inhibitor 3	395	-1.76	-4.57	-3.19
K02586	Gamma crystallin A	12401	-1.83	-5.2	-2.36
BC002008	Fatty acid binding protein 5	14299	-3.48	-3.26	-2.42
	Mkiaa1450 Protein	118	-2.48	-3	-3.29
	sodium shannel	1395	-2.99	-3.29	-2.38
BC022920	Expressed sequence AA408140	3694	-2.22	-3.5	-2.88
AB016768	R-spondin, thrombospondin-1-like domain	123	-3.03	-3.11	-1.84
X52128	T-complex protein 11	246	-1.71	-3.99	-2.11
AK037164	Translation initiation factor	1597	-2.17	-2.93	-2.67
BC024653	O-acyltransferase	2740	-1.81	-3.3	-2.4
NM_172296	Doublesex and mab-3	386	-1.95	-2.91	-2.46
AF020772	Karyopherin (importin) alpha 3	318	-1.15	-4.75	-1.39
L14569	Olfactory receptor 7B	43	1.05	-5.11	-3.22
D14423	Tachykinin 2	572	-2.06	-3.38	-1.81
AF156979	Arrestin 3	2920	-2.22	-2.72	-1.8
AY158991	Small proline-rich protein 2G	698	-1.81	-3.02	-1.86
BC012704	Carbonic anhydrase 4	9297	-2.21	-2.63	-1.81
AF032115	DnaJ (Hsp40) homolog	2192	-2.32	-2.55	-1.77

Top 50 genes with the greatest decrease in relative mRNA expression levels of regenerating lens compared to intact control lens 1, 2, and 3 weeks post-extracapsular surgery. For a better visual presentation of the regulated genes at 1, 2, and 3 weeks, the times that each gene is lowest is marked in red.

involved in transcription and protein synthesis and may be a key early event.

The overall pattern clearly follows two different biological processes that take place after the extracapsular operation. In the initial stages, there is EMT and considerable remodeling of the extracellular matrix. At later stages, a lens differentiation program takes over due to regeneration of lens fibers. This observation is also clear from a list of the top 50 differentially expressed genes that showed the greatest increase in mRNA levels across the different times after surgery relative to control lens (Table 1). Thrombospondin-1 (TSP-1) precursor showed the greatest fold-change increase. TSP-1 is a glycoprotein involved in the activation of TGF-β, which is considered to be the main inducing factor of EMT [27]. TSP-1 has been shown to accumulate during PCO and decline during fiber differentiation [27]. Other highly upregulated genes encode proteins that are involved in matrix remodeling, such as procollagen, TIMP-1, cathepsin, tenascin C, proteinases, and leucine-rich repeat containing protein (Table 1). Among the 50 genes that showed the greatest decrease in mRNA levels in the regenerating lens relative to the control (Table 2) are genes that encode structural proteins of differentiated lens fibers. The list includes several crystallins, phakinin, beaded filament structural protein, lens fiber membrane intrinsic protein, and lens fiber major intrinsic protein. Also, several regulatory genes, such as the homeo box NKX-2.2, the Kruppel factor 7, the cAMP responsive element binding protein, and NFAT are clustered with the lens fiber-specific ones (Table 2). In Table 1 and Table 2, the time with the highest (or lowest) regulation is highlighted in red. This was designed to help the reader to identify with a glance the times and the genes showing the most regulation. Interestingly, it becomes obvious that at week 2 we have the most severe regulation, positive or negative. These findings may eventually allow us to identify specific gene regulation programs involved in the distinct processes of EMT and fiber differentiation that take place during the process of mouse lens regeneration. The only genes that also coincide with cataract loci are the crystallin genes.

We further examined five general patterns of expression identified by correlating the clusters formed by the cluster

Table 3.

Main GO category	Number of genes in the category	Gene category	False discovery rate
Biological Process	10	Defense response	8.2E-03
	10	Response to biotic stimulus	1.6E-02
	4	Chemotaxis	3.3E-02
	4	Taxis	3.3E-02
	3	Cellular defense response	5.3E-02
	7	Immune response	7.9E-02
	2	Antigen processing	7.9E-02
	4	Response to wounding	7.9E-02
	4	Response to chemical substance	7.9E-02
	11	Response to external stimulus	7.9E-02
Cellular Component	31	Extracellular	3.9E-06
	28	Extracellular space	9.1E-06
	7	Lytic vacuole	1.7E-04
	7	Lysosome	1.7E-04
	7	Vacuole	3.1E-04
	2	Histone acetyltransferase complex	7.9E-02
Molecular Function	3	Cytokine binding	3.5E-02
	5	Cytokine activity	4.6E-02
	2	Interleukin receptor activity	7.9E-02
	2	Interleukin binding	7.9E-02
	2	Chemokine receptor binding	7.9E-02
	2	Chemokine activity	7.9E-02
	3	Exopeptidase activity	7.9E-02
	2	Chemoattractant activity	7.9E-02
	2	G-protein-coupled receptor binding	8.5E-02
	2	Growth factor binding	9.6E-02
	2	Carboxypeptidase activity	9.6E-02
	6	Receptor binding	9.6E-02

Gene ontology (GO) categories of the gene cluster displaying a weak uniform increase in relative mRNA levels of regenerating lens compared to intact control lens.

TABLE 4.

GenBank accession	Symbol	Description
BC010275	Arpc1b	Actin related protein 2/3 complex, subunit 1B
M10416	B2m	Beta-2 microglobulin
U89399	Coro1a	Coronin, actin binding protein 1A
S70244	Clu	Clusterin
U56819	Ccr2	Chemokine (C-C motif) receptor 2
AF237721	Col9a3	Procollagen, type IX, alpha 3
AF039391	Crym	Crystallin, mu
S69034	Ctsb	Cathepsin B
U74683	Ctsc	Cathepsin C
D88689	Flt1	FMS-like tyrosine kinase 1
AF254441	Gcn5l2	GCN5 general control of amino acid synthesis-like 2 (yeast)
BC016431	Leprel2	Leprecan-like 2
X62321	Grn	Granulin
AF267747	Gtf2i	General transcription factor II I
BC034217	H13	Histocompatibility 13
AB013095	Hebp1	Heme binding protein 1
U07741	Hexb	Hexosaminidase B
X05429	Ii	Ia-associated invariant chain
U53696	Il10rb	Interleukin 10 receptor, beta
M20658	Il1r1	Interleukin 1 receptor, type I
D16313	Krt1-15	Keratin complex 1, acidic, gene 15
X03491	Krt2-4	Keratin complex 2, basic, gene 4
J03881	Lamp1	Lysosomal membrane glycoprotein 1
M32018	Lamp2	Lysosomal membrane glycoprotein 2
AJ243857	Lhx9	LIM homeobox protein 9
AF139987	Limk1	LIM-domain containing, protein kinase
M89956	Lsp1	Lymphocyte specific 1
AF004874	Ltbp2	Latent transforming growth factor beta binding protein 2
AK007774	Ltbp3	Latent transforming growth factor beta binding protein 3
AJ298054	Blnk	B-cell linker
U47737	Ly6e	Lymphocyte antigen 6 complex, locus E
M34094	Mdk	Midkine
L11625	Mertk	C-mer proto-oncogene tyrosine kinase
S77350	Mglap	Matrix gamma-carboxyglutamate (gla) protein
M77226	Muc1	Mucin 1, transmembrane
AK036379	Ncf2	Neutrophil cytosolic factor 2
X57337	Pcolce	Procollagen C-proteinase enhancer protein
M74227	Ppic	Peptidylprolyl isomerase C
AF065933	Ccl2	Chemokine (C-C motif) ligand 2
BC032922	Sla	Src-like adaptor
X57413	Tgfb2	Transforming growth factor, beta 2
J03299	Trf	Transferring
BC011182	Zfp39	Zinc finger protein 39
X76696	Cd52	CD52 antigen
AF358138	Hcst	Hematopoietic cell signal transducer
AJ249987	Taf10	TAF10 RNA polymerase II, TATA box binding protein (TBP)-associated factor
AK018587	Batf	Basic leucine zipper transcription factor, ATF-like
AK076162	Litaf	LPS-induced TN factor
AF290973	Ifi30	Interferon gamma inducible protein 30
BC005532	Cndp2	CNDP dipeptidase 2 (metallopeptidase M20 family)
AK029988	Cxcl16	Chemokine (C-X-C motif) ligand 16
AF219141	Agtpbp1	ATP/GTP binding protein 1
AF393640	Srpx2	Sushi-repeat-containing protein, X-linked 2
AK007397	Adh6a	Alcohol dehydrogenase 6A (class V)
AF345635	Pir	Pirin
AJ421478	Cnbp2	Cellular nucleic acid binding protein 2
BC034522	Oplah	5-oxoprolinase (ATP-hydrolysing)
BC048078	AI428855	Expressed sequence AI428855
BC022145	BC022145	cDNA sequence BC022145
BC013712	BC013712	cDNA sequence BC013712
BC027331	P2ry6	Pyrimidinergic receptor P2Y, G-protein coupled, 6
AK007226	Atp2c1	ATPase, Ca++-sequestering
AK028285	Sulf1	Sulfatase 1
AK047568	Snph	Syntaphilin
U29501	Zfp75	Zinc finger protein 75
BC028661	Myo1g	Myosin IG
BC025046	Cdk8	Cyclin-dependent kinase 8

The gene cluster displaying a weak uniform increase in relative mRNA levels of regenerating lens compared to intact control lens.

analysis of gene expression profiles and functional clusters based on GO categories.

Weak uniform increase in RNA levels: In this group, the clustered genes showed a general pattern of a relatively slight increase in RNA levels throughout the regeneration process. In Table 3, the genes are divided according to main GO category, biological process, cellular component, and molecular function. Table 4 presents a general feature of this subgroup in that it contains genes involved in defense, response to injury, and extracellular matrix metabolism and also includes TGF-β and TGF-β-binding proteins, which are known mediators of EMT.

Strong uniform increase in RNA levels: As in the previous group, the genes in this cluster showed a general increase in RNA levels but more pronounced. These genes are involved in immune response, adhesion and remodeling, and processes that mediate injury and re-building of tissues after damage. Thrombospondins and disintegrins are included in the list (Table 5, Table 6).

Strong delayed increase in RNA levels: The mRNA levels of the genes in this group showed a sharp increase at week 2. Most of these genes are involved in cytoskeletal organization and negative regulation of transcription (Table 7, Table 8).

TABLE 5.

Main GO category	Number of genes in the category	Gene category	False discovery rate
Biological Process	17	Response to biotic stimulus	1.0E-06
	16	Defense response	1.2E-06
	14	Immune response	3.3E-06
	7	Humoral immune response	3.3E-06
	10	Response to pest/pathogen/parasite	2.4E-05
	18	Response to external stimulus	3.9E-04
	4	Complement activation	1.6E-03
	11	Cell adhesion	2.1E-03
	4	Humoral defense mechanism (sensu Vertebrata)	2.3E-03
	3	Antigen processing	3.3E-03
	11	Response to stress	4.7E-03
	3	Antigen presentation	5.1E-03
	3	Complement activation, classical pathway	5.1E-03
	4	Angiogenesis	6.2E-03
	4	Blood vessel development	1.0E-02
	2	Antigen presentation, exogenous antigen	1.2E-02
	2	Antigen processing, exogenous antigen via MHC class II	1.2E-02
	2	Cell wall catabolism	1.6E-02
	2	Regulation of angiogenesis	3.0E-02
	2	Cytolysis	4.9E-02
Cellular Component	45	Extracellular	4.7E-11
	41	Extracellular space	2.0E-10
	13	Extracellular matrix	1.1E-06
	2	Complement component C1q complex	1.9E-03
Molecular Function	10	Glycosaminoglycan binding	7.9E-10
	9	Heparin binding	5.7E-09
	4	Complement activity	4.3E-04
	9	Cell adhesion molecule activity	1.9E-03
	6	Defense/immunity protein activity	1.9E-03
	2	Lysozyme activity	4.2E-03
	3	Scavenger receptor activity	9.5E-03
	2	MHC class II receptor activity	1.0E-02
	5	Endopeptidase inhibitor activity	1.2E-02
	5	Protease inhibitor activity	1.2E-02
	6	Enzyme inhibitor activity	1.9E-02
	10	Enzyme regulator activity	1.9E-02
	2	Integrin binding	4.1E-02
	2	Insulin-like growth factor binding	6.7E-02
	2	Antimicrobial peptide activity	6.7E-02
	24	Signal transducer activity	6.7E-02

Gene Ontology (GO) categories of the gene cluster displaying a strong uniform increase in relative mRNA levels of regenerating lens compared to intact control lens.

TABLE 6.

GenBank accession	Symbol	Description
BC021539	Aif1	allograft inflammatory factor 1
AF212924	Ank3	ankyrin 3, epithelial
U72941	Anxa4	annexin A4
M73490	Apoe	apolipoprotein E
Y11758	Bgn	Biglycan
X58861	C1qa	complement component 1, q subcomponent, alpha polypeptide
X92959	C1qb	complement component 1, q subcomponent, beta polypeptide
X92960	C1qg	complement component 1, q subcomponent, gamma polypeptide
AF053757	C3ar1	complement component 3a receptor 1
BC030071	Calca	calcitonin/calcitonin-related polypeptide, alpha
X07411	Cbr2	carbonyl reductase 2
BC004076	Ccnd3	cyclin D3
X93035	Chi3l1	chitinase 3-like 1
AK052963	Col14a1	procollagen, type XIV, alpha 1
U49430	Cp	ceruloplasmin
BC002072	Cst3	cystatin C
AJ006033	Ctsk	cathepsin K
AJ223208	Ctss	cathepsin S
AK018713	Cyba	cytochrome b-245, alpha polypeptide
AF071068	Ddc	dopa decarboxylase
L33416	Ecm1	extracellular matrix protein 1
M26498	Edn2	endothelin 2
AF135252	Fbln2	fibulin 2
X60929	Fcgr3	Fc receptor, IgG, low affinity III
BC006783	Ctgf	connective tissue growth factor
BC004647	Flot1	flotillin 1
BC004724	Fn1	fibronectin 1
AF149059	Gclm	glutamate-cysteine ligase, modifier subunit
U05264	Lilrb4	leukocyte immunoglobulin-like receptor, subfamily B, member 4
V01527	H2-Ab1	histocompatibility 2, class II antigen A, beta 1
M18524	H2-D1	histocompatibility 2, D region locus 1
M69069	H2-D1	histocompatibility 2, D region locus 1
M36939	H2-Eb1	histocompatibility 2, class II antigen E beta
X56790	Cyr61	cysteine rich protein 61
X81627	Lcn2	lipocalin 2
L04264	Lox	lysyl oxidase
BC002069	Lyzs	lysozyme
X51547	Lzp-s	P lysozyme structural
AF061272	Clecsf8	C-type (calcium dependent, carbohydrate recognition domain) lectin, superfamily member 8
X97650	Myo1f	myosin IF
U83172	Pirb	paired-Ig-like receptor B
M33960	Serpine1	serine (or cysteine) proteinase inhibitor, clade E, member 1
D37837	Lcp1	lymphocyte cytosolic protein 1
AK002410	Plscr2	phospholipid scramblase 2
U33626	Pml	promyelocytic leukemia
AK079915	Lgals3bp	lectin, galactoside-binding, soluble, 3 binding protein
U57999	Psap	prosaposin
S72304	Rab34	RAB34, member of RAS oncogene family
AK004165	Rgs5	regulator of G-protein signaling 5
U58886	Sh3gl2	SH3-domain GRB2-like 2
BC013651	Serpina3n	serine (or cysteine) proteinase inhibitor, clade A, member 3N
X70946	Serpine2	serine (or cysteine) proteinase inhibitor, clade E, member 2
AK010442	Syngr1	synaptogyrin 1
M64866	Thbs2	thrombospondin 2
M17243	Timp1	tissue inhibitor of metalloproteinase 1
D90343	Tnc	tenascin C
AF077829	Tyrobp	TYRO protein tyrosine kinase binding protein
U42327	Vcam1	vascular cell adhesion molecule 1
AF175282	Adamts8	a disintegrin-like and metalloprotease (reprolysin type) with thrombospondin type 1 motif, 8
D13664	Postn	periostin, osteoblast specific factor
AF350047	Rgs3	regulator of G-protein signaling 3
BC023008	Clecsf10	C-type (calcium dependent, carbohydrate recognition domain) lectin, superfamily member 10
BC003482	Tm4sf7	transmembrane 4 superfamily member 7
AY082484	Ifitm3	interferon induced transmembrane protein 3
BC019764	Ube1dc1	ubiquitin-activating enzyme E1-domain containing 1
AK007397	Adh6a	alcohol dehydrogenase 6A (class V)
BC027425	Ms4a6b	membrane-spanning 4-domains, subfamily A, member 6B
AK010084	2310067E08Rik	RIKEN cDNA 2310067E08 gene
BC013494	Cyp4f18	cytochrome P450, family 4, subfamily f, polypeptide 18
AK008652	Ms4a6c	membrane-spanning 4-domains, subfamily A, member 6C
BC016551	Msr2	macrophage scavenger receptor 2
AF213458	Trem2	triggering receptor expressed on myeloid cells 2
BC026375	Gpnmb	glycoprotein (transmembrane) nmb
AJ308965	Psip1	PC4 and SFRS1 interacting protein 1
AF398968	Asb7	ankyrin repeat and SOCS box-containing protein 7
AK033038	Oosp1	oocyte secreted protein 1
AF290914	Stab1	stabilin 1

The gene cluster displaying a strong uniform increase in relative mRNA levels of regenerating lens compared to intact control lens.

Table 7.

Main GO category	Number of genes in the category	Gene category	False discovery rate
Biological Process	6	negative regulation of transcription	7.8E-02
	5	negative regulation of transcription, DNA-dependent	9.7E-02
	9	cytoskeleton organization and biogenesis	9.7E-02

Gene Ontology categories of the gene cluster displaying a strong increase in relative mRNA levels late during lens regeneration compared to intact control lens.

Table 8.

GenBank accession	Symbol	Description
U76732	Adh7	Alcohol dehydrogenase 7 (class IV), mu or sigma polypeptide
U88623	Aqp4	Aquaporin 4
L07918	Arhgdib	Rho, GDP dissociation inhibitor (GDI) beta
AC002397	Bcap37	B-cell receptor-associated protein 37
D16432	Cd63	Cd63 antigen
M64278	Chga	Chromogranin A
X04591	Ckb	Creatine kinase, brain
AB033123	Ctbp2	C-terminal binding protein 2
X94998	Fmod	Fibromodulin
S71213	Gnai2	Guanine nucleotide binding protein, alpha inhibiting 2
M96645	Gp38	Glycoprotein 38
AF027505	Baiap1	BAI1-associated protein 1
D16464	Hes1	Hairy and enhancer of split 1 (Drosophila)
M10062	Iap	Intracisternal A particles
M60523	Idb3	Inhibitor of DNA binding 3
BC003804	Ifit3	Interferon-induced protein with tetratricopeptide repeats 3
AK011790	Igfbp2	Insulin-like growth factor binding protein 2
X69902	Itga6	Integrin alpha 6
M64228	Kcnb1	Potassium voltage gated channel, Shab-related subfamily, member 1
AB023656	Kif1b	Kinesin family member 1B
AF202892	Kif21a	Kinesin family member 21A
D16313	Krt1-15	Keratin complex 1, acidic, gene 15
M13805	Krt1-17	Keratin complex 1, acidic, gene 17
U55060	Lgals9	Lectin, galactose binding, soluble 9
AF367720	Lrp1	Low density lipoprotein receptor-related protein 1
X66983	Mak	Male germ cell-associated kinase
AF047714	Trpm1	Transient receptor potential cation channel, subfamily M, member 1
M36411	Mpv17	Mpv17 transgene, kidney disease mutant
AJ249706	Myo10	Myosin X
AK077116	Naga	N-acetyl galactosaminidase, alpha
X61450	Napb	N-ethylmaleimide sensitive fusion protein attachment protein beta
X61455	Napb	N-ethylmaleimide sensitive fusion protein attachment protein beta
S40532	Nhlh2	Nescient helix loop helix 2
AF219626	Ninj1	Ninjurin 1
AJ006803	Nrxn2	Neurexin II
U79523	Pam	Peptidylglycine alpha-amidating monooxygenase
AF023529	Pde1a	Phosphodiesterase 1A, calmodulin-dependent
BC005661	Pgam1	Phosphoglycerate mutase 1
L43371	Ppap2a	Phosphatidic acid phosphatase 2a
X58990	Ppib	Peptidylprolyl isomerase B
BC004730	Psmb10	Proteasome (prosome, macropain) subunit, beta type 10
AB001607	Ptgis	Prostaglandin I2 (prostacyclin) synthase
AK088005	Ptma	Prothymosin alpha
S52353	Ptn	Pleiotrophin
AK050418	Rp2h	Retinitis pigmentosa 2 homolog (human)
D43805	Cxcl12	Chemokine (C-X-C motif) ligand 12

Weak early decrease in RNA levels: The main characteristic of this group was that the genes are involved in nucleic acid biosynthesis and ribosomal function. This result suggests that during the early events of repair, there is a general inhibition of transcriptional and translational events (Table 9, Table 10).

Strong uniform decrease in RNA levels: The genes in this cluster are involved in sensory organ development, perception of light, and the structural components of the lens (Table 11, Table 12). mRNA levels for the crystallins and other structural proteins of the lens, such as phakinin, are severely decreased indicating that lens fiber differentiation is not at its final stages during the repair process. Naturally, the drop in RNA levels of some genes in this group becomes less severe with the later stages of lens fiber differentiation (3 weeks post-lentectomy).

Verification of expression by quantitative real-time polymerase chain reaction: We selected ten genes to verify their expression by quantitative real-time polymerase chain reaction (QPCR). The selected genes showed different patterns of expression in the microarray experiments. TIMP1 showed a strong uniform increase in RNA levels, lysozyme showed strong increase at week 2, ceruloplasmin showed a weak uniform increase and γB-crystallin showed strong uniform decrease in RNA levels. Others showed not much variation and had lower levels. Ratios observed in microarray experiments

Table 8. Continued.

GenBank accession	Symbol	Description
M74773	Spnb2	Spectrin beta 2
U30709	Stat3	Signal transducer and activator of transcription 3
U55862	Tia1	Cytotoxic granule-associated RNA binding protein 1
M93954	Timp2	Tissue inhibitor of metalloproteinase 2
U41741	Usf1	Upstream transcription factor 1
U80078	Zfp148	Zinc finger protein 148
AJ316580	Mgll	Monoglyceride lipase
U43206	Pbp	Phosphatidylethanolamine binding protein
AF033116	Zfhx1b	Zinc finger homeobox 1b
AK020876	Nubp1	Nucleotide binding protein 1
AF128236	Psg18	Pregnancy specific glycoprotein 18
AB071988	H2afy	H2A histone family, member Y
AY133242	Ahi1	Abelson helper integration site
AF239886	Espn	Espin
AK010636	MGI:1929282	Telomerase binding protein, p23
BC007177	Ccnl1	Cyclin L1
BC014726	Sertad2	SERTA domain containing 2
AK088173	Nek7	NIMA (never in mitosis gene a)-related expressed kinase 7
AK075861	Sirt3	Sirtuin 3 (silent mating type information regulation 2, homolog) 3 (S. cerevisiae)
BC031854	D14Ertd449e	DNA segment, Chr 14, ERATO Doi 449, expressed
AK009412	Srp19	Signal recognition particle 19
AK017655	Luc7l	Luc7 homolog (S. cerevisiae)-like
BC027328	Bst2	Bone marrow stromal cell antigen 2
AK005050	Dhdh	Dihydrodiol dehydrogenase (dimeric)
BC052406	Brunol6	Bruno-like 6, RNA binding protein (Drosophila)
AY055832	Mtmr2	Myotubularin related protein 2
BC002262		Mus musculus expressed sequence AI428795, mRNA
AF130313	Nckipsd	NCK interacting protein with SH3 domain
BC021457	Slmap	Sarcolemma associated protein
AF252281	Klhl1	Kelch-like 1 (Drosophila)
AY013783	Pcdhb21	Protocadherin beta 21
AF296412	Aipl1	Aryl hydrocarbon receptor-interacting protein-like 1
AY078170	Dph2l1	Diptheria toxin resistance protein required for diphthamide biosynthesis (Saccharomyces)-like 1
BC019406	Bbox1	Butyrobetaine (gamma), 2-oxoglutarate dioxygenase 1 (gamma-butyrobetaine hydroxylase)
AF403039	MGI:2183445	SPRY domain-containing SOCS box 4
BC027170	C79267	Expressed sequence C79267
BC027407	Zfp472	Zinc finger protein 472
BC017130	Pja2	Praja 2, RING-H2 motif containing
BC003885	BC003885	cDNA sequence BC003885
BC027194	Golph3l	Golgi phosphoprotein 3-like
BC027279	Blvrb	Biliverdin reductase B (flavin reductase (NADPH))
AK044042	Cpne5	Copine V
AK075830	Usp7	UUbiquitin specific protease 7
AK030085	D2Ertd485e	DNA segment, Chr 2, ERATO Doi 485, expressed

The gene cluster displaying a strong increase in relative mRNA levels late during lens regeneration compared to intact control lens.

TABLE 9.

Main GO category	Number of genes in the category	Gene category	False discovery rate
Biological Process	16	Macromolecule biosynthesis	2.9E-03
	17	Biosynthesis	5.3E-03
	12	Protein biosynthesis	6.1E-03
	2	RNA elongation	2.8E-02
	3	Purine ribonucleoside triphosphate biosynthesis	5.3E-02
	3	Purine nucleoside triphosphate biosynthesis	5.3E-02
	3	Ribonucleoside triphosphate biosynthesis	5.3E-02
	7	Perception of abiotic stimulus	5.3E-02
	7	Sensory perception	5.3E-02
	3	Purine ribonucleoside triphosphate metabolism	5.3E-02
	3	Ribonucleoside triphosphate metabolism	5.3E-02
	3	Nucleoside triphosphate biosynthesis	5.3E-02
	5	Perception of chemical substance	5.3E-02
	5	Chemosensory perception	5.3E-02
	3	Purine nucleoside triphosphate metabolism	5.3E-02
	14	G-protein coupled receptor protein signaling pathway	5.8E-02
	7	Perception of external stimulus	5.8E-02
	3	Purine ribonucleotide biosynthesis	5.8E-02
	3	Nucleoside triphosphate metabolism	5.8E-02
	3	Purine nucleotide biosynthesis	6.9E-02
	3	Ribonucleotide biosynthesis	7.1E-02
	2	Phosphoenolpyruvate-dependent sugar phosphotransferase system	7.6E-02
	3	Purine ribonucleotide metabolism	7.6E-02
	3	Purine nucleotide metabolism	7.8E-02
	3	Ribonucleotide metabolism	7.8E-02
	2	Oxidative phosphorylation	8.7E-02
	2	ATP biosynthesis	9.8E-02
	2	Nucleoside phosphate metabolism	9.8E-02
Cellular Component	10	Ribosome	2.0E-03
	12	Ribonucleoprotein complex	2.0E-03
	14	Mitochondrion	1.2E-02
	3	Small ribosomal subunit	5.3E-02
	2	Transport vesicle	5.3E-02
	3	Organellar ribosome	5.8E-02
	3	Mitochondrial ribosome	5.8E-02
	3	Mitochondrial matrix	9.8E-02
	2	Mitochondrial large ribosomal subunit	9.9E-02
	2	Organellar large ribosomal subunit	9.9E-02
Molecular Function	10	Structural constituent of ribosome	1.1E-03
	13	Structural molecule activity	1.7E-02
	10	RNA binding	2.2E-02
	4	Hydrogen ion transporter activity	7.8E-02
	4	Monovalent inorganic cation transporter activity	7.8E-02
	2	Oxidoreductase activity, acting on heme group of donors, oxygen as acceptor	7.8E-02
	2	Cytochrome-c oxidase activity	7.8E-02
	2	Oxidoreductase activity, acting on heme group of donors	7.8E-02
	2	Heme-copper terminal oxidase activity	7.8E-02
	2	DNA dependent ATPase activity	8.1E-02
	2	Damaged DNA binding	9.7E-02

Gene ontology (GO) categories of the gene cluster displaying a weak decrease in relative mRNA levels early during lens regeneration compared to intact control lens.

TABLE 10.

GenBank accession	Symbol	Description
AF104416	Aqp3	aquaporin 3
BC011291	Arbp	acidic ribosomal phosphoprotein P0
X52940	Cox7c	cytochrome c oxidase, subunit VIIc
X53599	Fmn	formin
U38498	Gng5	guanine nucleotide binding protein (G protein), gamma 5 subunit
AF319526	Gstm2	glutathione S-transferase, mu 2
U96116	Hadh2	hydroxyacyl-Coenzyme A dehydrogenase type II
D63663	Pwwp1	PWWP domain containing 1
U60001	Hint1	histidine triad nucleotide binding protein 1
U12791	Hmgcs2	3-hydroxy-3-methylglutaryl-Coenzyme A synthase 2
AK004568	Rps2	ribosomal protein S2
X68193	Nme2	expressed in nonmetastatic cells 2, protein
AF102540	Olfr61	olfactory receptor 61
AK011242	Rad51	RAD51 homolog (S. cerevisiae)
AK012580	Rpl18	ribosomal protein L18
AK086805	Mrpl23	mitochondrial ribosomal protein L23
L08651	Rpl29	ribosomal protein L29
X80899	Cox7a2l	cytochrome c oxidase subunit VIIa polypeptide 2-like
AF042139	Ssa2	Sjogren syndrome antigen A2
BC010807	Tcea3	transcription elongation factor A (SII), 3
U60150	Vamp2	vesicle-associated membrane protein 2
BC037541	Lynx1	Ly6/neurotoxin 1
AF093260	Homer2	homer homolog 2 (Drosophila)
X76772	Rps3	ribosomal protein S3
AK008036	Atp5l	ATP synthase, H+ transporting, mitochondrial F0 complex, subunit g
BC012241	Atp5o	ATP synthase, H+ transporting, mitochondrial F1 complex, O subunit
AF177399	Dkkl1	dickkopf-like 1
BC011162	Ncald	neurocalcin delta
AF119676	Rab25	RAB25, member RAS oncogene family
AK002585	Fxyd1	FXYD domain-containing ion transport regulator 1
AK030225	Cyb561d2	cytochrome b-561 domain containing 2
AK014963	Xrcc2	X-ray repair complementing defective repair in Chinese hamster cells 2
AF124425	Cldn10	claudin 10
AB024448	Jph2	junctophilin 2
AK028318	Sv2a	synaptic vesicle glycoprotein 2 a
AK018778	Gng13	guanine nucleotide binding protein 13, gamma
AK003225	Mrpl54	mitochondrial ribosomal protein L54
BC027511	Lsm7	LSM7 homolog, U6 small nuclear RNA associated (S. cerevisiae)
AF230339	Znrd1	zinc ribbon domain containing, 1
AK003341	Chchd5	coiled-coil-helix-coiled-coil-helix domain containing 5
BC027546	Mrps21	mitochondrial ribosomal protein S21
AK028011	Ndufc1	NADH dehydrogenase (ubiquinone) 1, subcomplex unknown, 1
AK010329	Mrpl11	mitochondrial ribosomal protein L11
BC024346	MGI:1913699	mitochondria-associated protein involved in GMCSF signal transduction
AK088737	Rplp2	ribosomal protein, large P2
AK003223	Dpm3	dolichyl-phosphate mannosyltransferase polypeptide 3
AK003192	Ict1	immature colon carcinoma transcript 1
BC030905	Ascc1	activating signal cointegrator 1 complex subunit 1
AK008201	Ndufa11	NADH dehydrogenase (ubiquinone) 1 alpha subcomplex 11
AB093231	Tln2	talin 2
AY071834	Optn	optineurin
AK005562	Eml2	echinoderm microtubule associated protein like 2
AF319173	Psca	prostate stem cell antigen
AK006855	MGI:1920610	actin-related protein T1
BC016253	Man2c1	mannosidase, alpha, class 2C, member 1
AB046537	Pi16	protease inhibitor 16
AK049110	D15Ertd735e	DNA segment, Chr 15, ERATO Doi 735, expressed
AJ421478	Cnbp2	cellular nucleic acid binding protein 2
AK012695	Mgea5	meningioma expressed antigen 5 (hyaluronidase)
AK020927	Rdh12	retinol dehydrogenase 12
AB053477	Abtb1	ankyrin repeat and BTB (POZ) domain containing 1
AJ278462	Mmp1a	matrix metalloproteinase 1a (interstitial collagenase)
X04652	Hist2h4	histone 2, H4
AF425084	Serpinb6c	serine (or cysteine) proteinase inhibitor, clade B, member 6c
AF372838	Rdh9	retinol dehydrogenase 9
BC031759	MGI:2135937	SH3-binding kinase

Table 10. Continued.

GenBank accession	Symbol	Description
BC034872	Gpr18	G protein-coupled receptor 18
AK079337	Baalc	brain and acute leukemia, cytoplasmic
AK029205	V1rc15	vomeronasal 1 receptor, C15
AK031458	AI428795	expressed sequence AI428795
AB091829	MGI:2384865	O-acetyltransferase
AK085987	Mtr	5-methyltetrahydrofolate-homocysteine methyltransferase
AY277588	MGI:2668443	retinal short chain dehydrogenase reductase 2
AY317805	Olfr684	olfactory receptor 684
AK033012	Npat	nuclear protein in the AT region
AF357887	Dusp15	dual specificity phosphatase-like 15
AY073826	Olfr747	olfactory receptor 747
AY073750	Olfr1265	olfactory receptor 1265
AY073749	Olfr1495	olfactory receptor 1495
AY073644	Olfr1231	olfactory receptor 1231
AY073624	Olfr1261	olfactory receptor 1261
AY073578	Olfr530	olfactory receptor 530
AY073509	Olfr1030	olfactory receptor 1030
AY073501	Olfr703	olfactory receptor 703
AY073438	Olfr1131	olfactory receptor 1131
AY073304	Olfr1238	olfactory receptor 1238
AY073177	Olfr1377	olfactory receptor 1377
AF171073	Ppia	peptidylprolyl isomerase A
BC034068	BC034068	cDNA sequence BC034068
AK047412	AU020772	expressed sequence AU020772
BC049929	Ddx11	DEAD/H box polypeptide 11 (CHL1-like helicase homolog, S. cerevisiae)
L38438	Ndufs6	NADH dehydrogenase (ubiquinone) Fe-S protein 6

The gene cluster displaying a weak decrease in relative mRNA levels early during lens regeneration compared to intact control lens.

Table 11.

Main GO category	Number of genes in the category	Gene category	False discovery rate
Biological Process	7	Sensory organ development	1.4E-09
	7	Peripheral nervous system development	9.6E-09
	5	Vision	9.0E-03
	5	Perception of light	1.1E-02
	5	Response to light	1.1E-02
	5	Response to radiation	1.4E-02
	8	Neurogenesis	1.5E-02
	2	Mo-molybdopterin cofactor biosynthesis	1.6E-02
	2	Mo-molybdopterin cofactor metabolism	1.6E-02
	2	Pteridine and derivative biosynthesis	4.1E-02
	2	Pteridine and derivative metabolism	4.8E-02
	2	Aromatic compound biosynthesis	5.5E-02
Cellular Component	29	Cytoplasm	9.5E-02
Molecular Function	7	Structural constituent of eye lens	9.6E-09

Gene Ontology (GO) categories of the gene cluster displaying a strong uniform decrease in relative mRNA levels of regenerating lens compared to intact control lens.

Table 12.

GenBank accession	Symbol	Description
AF072815	Aldh3a1	Aldehyde dehydrogenase family 3, subfamily A1
AF087654	Aqp5	Aquaporin 5
Y13606	Bfsp1	Beaded filament structural protein in lens-CP94
BC012704	Car4	Carbonic anhydrase 4
BC021649	Creb1	cAMP responsive element binding protein 1

Table 12. Continued.

GenBank accession	Symbol	Description
AJ239052	Cryba1	Crystallin, beta A1
AK053869	Crybb1	Crystallin, beta B1
AJ272229	Crybb3	Crystallin, beta B3
Z22573	Crygb	Crystallin, gamma B
M64544	Crygc	Crystallin, gamma C
AJ224342	Crygd	Crystallin, gamma D
AF032115	Dnajc5	DnaJ (Hsp40) homolog, subfamily C, member 5
AF047542	Cyp2c37	Cytochrome P450, family 2. subfamily c, polypeptide 37
AF104312	Hao1	Hydroxyacid oxidase 1, liver
S67000	Hdc	Histidine decarboxylase
M81659	Hoxa10	Homeo box A10
U03562	Hspb1	Heat shock protein 1
BC002008	Fabp5	Fatty acid binding protein 5, epidermal
AF020772	Kpna3	Karyopherin (importin) alpha 3
AJ243857	Lhx9	LIM homeobox protein 9
AF099938	C1qr1	Complement component 1, q subcomponent, receptor 1
AK002719	Mocs2	Molybdenum cofactor synthesis 2
U36576	Nfatc2	Nuclear factor of activated T-cells, cytoplasmic, Calcineurin-dependent 2
S83259	Nkx2-2	NK2 transcription factor related, locus 2 (Drosophila)
S81982	Nos1	Nitric oxide synthase 1, neuronal
U85786	Scn1b	Sodium channel, voltage-gated, type I, beta polypeptide
BC005434	Serpinb5	Serine (or cysteine) proteinase inhibitor, clade B, member 5
AY158991	Sprr2g	Small proline-rich protein 2G
U21110	Stat5b	Signal transducer and activator of transcription 5B
D14423	Tac2	Tachykinin 2
X52128	Tcp11	T-complex protein 11
U90889	Tkt	Transketolase
AK031386	D15Mit260	DNA Segment, Chr 15 Massachusetts Institute of Technology 260
AF302077	Mell1	Mel transforming oncogene-like 1
AY038025	Ngef	Neuronal guanine nucleotide exchange factor
AB021967	Igsf4a	Immunoglobulin superfamily, member 4A
AF334607	Dnase2b	Deoxyribonuclease II beta
AK003904	Slurp1	Secreted Ly6/Plaur domain containing 1
BC004057	Tacc2	Transforming, acidic coiled-coil containing protein 2
AF117382	Hic2	Hypermethylated in cancer 2
AF072881	Wsb2	WD repeat and SOCS box-containing 2
BC047277	Stk35	Serine/threonine kinase 35
AK002226	Lypdc2	Ly6/Plaur domain containing 2
AK006330	Gpr160	G protein-coupled receptor 160
AF320075	Nkg7	Matural killer cell group 7 sequence
AK012971	Lrriq2	Leucine-rich repeats and IQ motif containing 2
BC003884	Pacsin3	Protein kinase C and casein kinase substrate in neurons 3
AB037890	Sf3b1	Splicing factor 3b, subunit 1
BC004700	Klf7	Kruppel-like factor 7 (ubiquitous)
BC029689	Tdrd7	Tudor domain containing 7
BC022920	Dhx32	DEAH (Asp-Glu-Ala-His) box polypeptide 32
AJ304860	Bfsp2	Beaded filament structural protein 2, phakinin
AF391758	Vsx1	Visual system homeobox 1 homolog (zebrafish)
AF277385	MGI:2150387	Prostatic steroid binding protein C1
AF156979	Arr3	Arrestin 3, retinal
AB016768	MGI:2183426	Thrombospondin type 1 domain containing gene
BC032251	Bai3	Brain-specific angiogenesis inhibitor 3
AK080732	Kcnj14	Potassium inwardly-rectifying channel, subfamily J, member 14
M55171	Rho	Rhodopsin
BC024653	Oact1	O-acyltransferase (membrane bound) domain containing 1
AK089408	F730023N20	Hypothetical protein F730023N20
AK017800	Clic5	Chloride intracellular channel 5
AK037164	Eif5b	Eukaryotic translation initiation factor 5B
AF309072	Lctl	Lactase-like
AK032362	Usp32	Ubiquitin specific protease 32
L14569	Olfr144	Olfactory receptor 144
U08095	Krt1-12	Keratin complex 1, acidic, gene 12
BC029696	Dpp10	Dipeptidylpeptidase 10

The gene cluster displaying a strong uniform decrease in relative mRNA levels of regenerating lens compared to intact control lens.

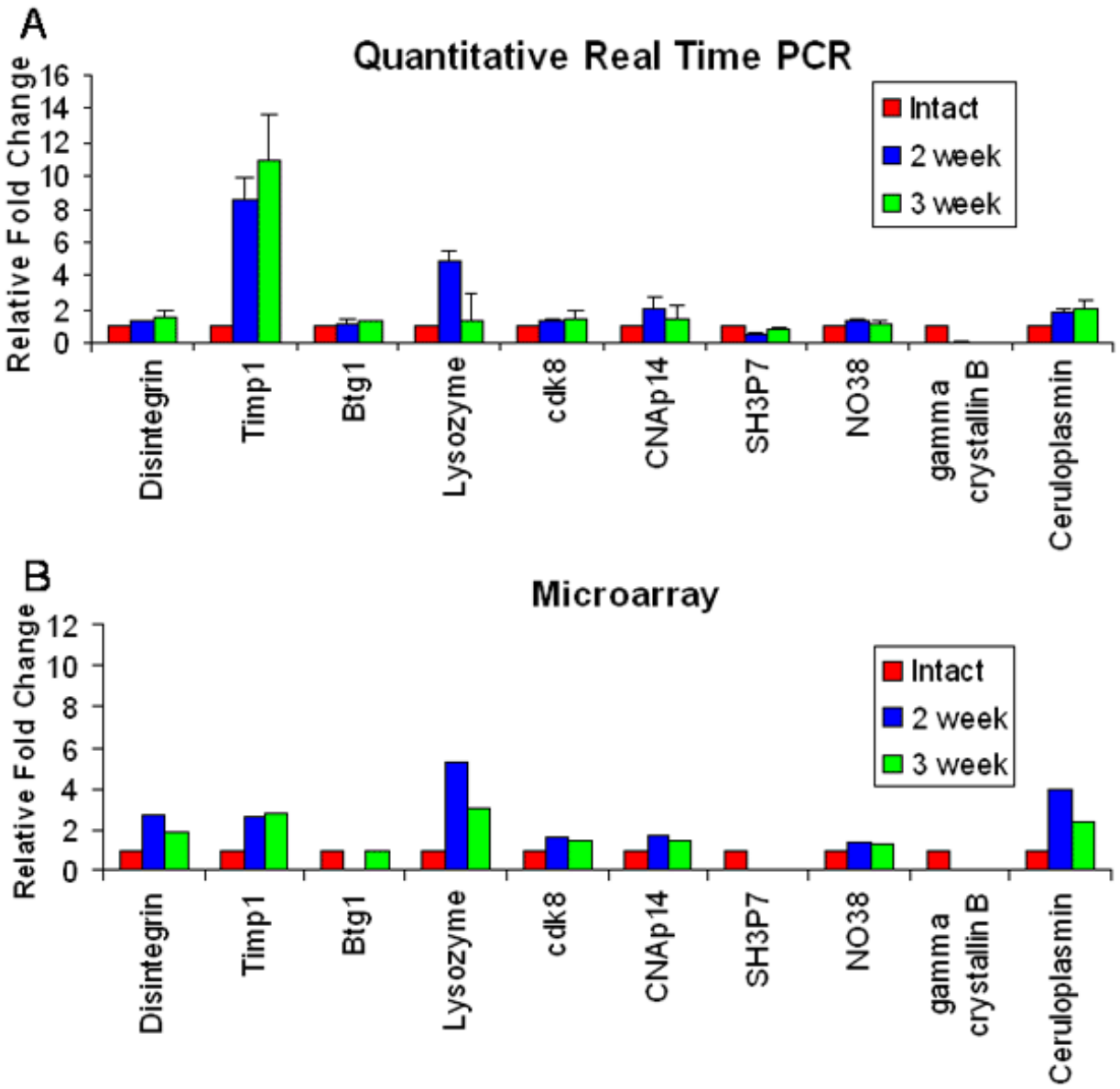

C:

	Microarray			Quantitative real time PCR		
Gene	Intact	2 week	3 week	Intact	2 week	3 week
Disintegrin	1	2.69	1.93	1	1.29	1.54
Timp1	1	2.62	2.75	1	8.56	10.87
Btg1	1	-1.3	1.02	1	1.2	1.3
Lysozyme	1	5.29	3.12	1	4.9	1.3
Cdk8	1	1.62	1.46	1	1.33	1.49
CNAp14	1	1.73	1.49	1	2.13	1.49
SH3P7	1	-1.88	-1.46	1	0.56	0.73
NO38	1	1.38	1.26	1	1.28	1.14
γB-Crystallin	1	-1.53	-2.06	1	0.03	0.007
Ceruloplasmin	1	4.01	2.39	1	1.77	2.04

Figure 4. QPCR analysis (**A**) of ten selected genes and the corresponding data from the microarray analysis (**B**). The expression values of lens mRNA at 2 and 3 weeks post-surgery are compared with lens mRNA from the non-operated eye (value set at 1). **C**: The values between the two methods.

for low expressed genes are most likely more variable for overall poorly expressed genes than for highly expressed genes. However, since we are using the statistical significance as the main criteria for identifying differentially expressed genes, such higher variability will be accounted for. That is, genes with higher variability in observed ratios will have lower statistical significance than genes with low variability ratios. Therefore, the statistical significance of low-expressed genes has been implicitly adjusted in our analysis and the statistically significant genes have equal chance of being false positives regardless of the overall level of expression. Nevertheless, we also decided to test such genes. As seen in Figure 4, expression of these genes as examined by QPCR was in excellent agreement with the microarray data. The housekeeping gene ATP synthase, epsilon subunit was used as the reference. This gene was found to have no differential expression in our microarray analysis and showed no differential expression in the QPCR experiments as well.

The mouse model for lens regeneration that we have described previously [6] is a valuable one because both EMT and lens fiber differentiation take place. Specifically, while the capsular bag is filled gradually with fibers, EMT is seen during the early stages and diminishes later. This has led us to utilize this model and examine global gene expression in order to associate clustered genes with both processes and identify new genes and networks. The availability of mutant mice will supplement these studies. By extensive genomic studies with mice lacking genes involved in EMT or lens fiber differentiation, the patterns of gene expression reported in this study could be sorted out in order to identify the role and regulation of known and novel genes involved in these processes. Extension of these studies, therefore, will lead to the establishment of databases and will provide indispensable and long-sought animal models for approaching PCO at the genetic level. At the same time, these studies will complement databases related to ocular bioinformatics [28-34].

ACKNOWLEDGEMENTS

This research was supported in part by NEI grant EY10540 to PAT.

REFERENCES

1. Del Rio-Tsonis K, Tsonis PA. Eye regeneration at the molecular age. Dev Dyn 2003; 226:211-24.
2. Tsonis PA, Del Rio-Tsonis K. Lens and retina regeneration: transdifferentiation, stem cells and clinical applications. Exp Eye Res 2004; 78:161-72.
3. Freeman G. Lens regeneration from the cornea in Xenopus laevis. J Exp Zool 1963; 154:39-65.
4. Gwon AE, Gruber LJ, Mundwiler KE. A histologic study of lens regeneration in aphakic rabbits. Invest Ophthalmol Vis Sci 1990; 31:540-7.
5. Gwon A, Gruber LJ, Mantras C. Restoring lens capsule integrity enhances lens regeneration in New Zealand albino rabbits and cats. J Cataract Refract Surg 1993; 19:735-46.
6. Call MK, Grogg MW, Del Rio-Tsonis K, Tsonis PA. Lens regeneration in mice: implications in cataracts. Exp Eye Res 2004; 78:297-9.
7. Lois N, Dawson R, McKinnon AD, Forrester JV. A new model of posterior capsule opacification in rodents. Invest Ophthalmol Vis Sci 2003; 44:3450-7.
8. Lois N, Taylor J, McKinnon AD, Forrester JV. Posterior capsule opacification in mice. Arch Ophthalmol 2005; 123:71-7.
9. Ibaraki N. A brighter future for cataract surgery. Nat Med 1997; 3:958-60.
10. Duncan G, Wormstone IM, Liu CS, Marcantonio JM, Davies PD. Thapsigargin-coated intraocular lenses inhibit human lens cell growth. Nat Med 1997; 3:1026-8.
11. Lee EH, Joo CK. Role of transforming growth factor-beta in transdifferentiation and fibrosis of lens epithelial cells. Invest Ophthalmol Vis Sci 1999; 40:2025-32.
12. Lovicu FJ, Schulz MW, Hales AM, Vincent LN, Overbeek PA, Chamberlain CG, McAvoy JW. TGFbeta induces morphological and molecular changes similar to human anterior subcapsular cataract. Br J Ophthalmol 2002; 86:220-6.
13. Wormstone IM, Tamiya S, Anderson I, Duncan G. TGF-beta2-induced matrix modification and cell transdifferentiation in the human lens capsular bag. Invest Ophthalmol Vis Sci 2002; 43:2301-8.
14. Iscove NN, Barbara M, Gu M, Gibson M, Modi C, Winegarden N. Representation is faithfully preserved in global cDNA amplified exponentially from sub-picogram quantities of mRNA. Nat Biotechnol 2002; 20:940-3.
15. Guo J, Sartor M, Karyala S, Medvedovic M, Kann S, Puga A, Ryan P, Tomlinson CR. Expression of genes in the TGF-beta signaling pathway is significantly deregulated in smooth muscle cells from aorta of aryl hydrocarbon receptor knockout mice. Toxicol Appl Pharmacol 2004; 194:79-89.
16. Karyala S, Guo J, Sartor M, Medvedovic M, Kann S, Puga A, Ryan P, Tomlinson CR. Different global gene expression profiles in benzo[a]pyrene- and dioxin-treated vascular smooth muscle cells of AHR-knockout and wild-type mice. Cardiovasc Toxicol 2004; 4:47-73.
17. Sartor M, Schwanekamp J, Halbleib D, Mohamed I, Karyala S, Medvedovic M, Tomlinson CR. Microarray results improve significantly as hybridization approaches equilibrium. Biotechniques 2004; 36:790-6.
18. Wolfinger RD, Gibson G, Wolfinger ED, Bennett L, Hamadeh H, Bushel P, Afshari C, Paules RS. Assessing gene significance from cDNA microarray expression data via mixed models. J Comput Biol 2001; 8:625-37.
19. Benjamini Y, Hochberg Y. Controlling the false discovery rate: a practical and powerful approach to multiple testing. Journal of the Royal Statistical Society. Series B (Statistical Methodology) 1995; 57:289-300.
20. Reiner A, Yekutieli D, Benjamini Y. Identifying differentially expressed genes using false discovery rate controlling procedures. Bioinformatics 2003; 19:368-75.
21. Medvedovic M, Sivaganesan S. Bayesian infinite mixture model based clustering of gene expression profiles. Bioinformatics 2002; 18:1194-206.
22. Medvedovic M, Yeung KY, Bumgarner RE. Bayesian mixture model based clustering of replicated microarray data. Bioinformatics 2004; 20:1222-32.
23. Eisen MB, Spellman PT, Brown PO, Botstein D. Cluster analysis and display of genome-wide expression patterns. Proc Natl Acad Sci U S A 1998; 95:14863-8.
24. Ashburner M, Ball CA, Blake JA, Botstein D, Butler H, Cherry JM, Davis AP, Dolinski K, Dwight SS, Eppig JT, Harris MA, Hill DP, Issel-Tarver L, Kasarskis A, Lewis S, Matese JC, Richardson JE, Ringwald M, Rubin GM, Sherlock G. Gene

ontology: tool for the unification of biology. The Gene Ontology Consortium. Nat Genet 2000; 25:25-9.
25. Hosack DA, Dennis G Jr, Sherman BT, Lane HC, Lempicki RA. Identifying biological themes within lists of genes with EASE. Genome Biol 2003; 4:R70.
26. Pfaffl MW. A new mathematical model for relative quantification in real-time RT-PCR. Nucleic Acids Res 2001; 29:e45.
27. Saika S, Miyamoto T, Ishida I, Barbour WK, Ohnishi Y, Ooshima A. Accumulation of thrombospondin-1 in post-operative capsular fibrosis and its down-regulation in lens cells during lens fiber formation. Exp Eye Res 2004; 79:147-56.
28. Wistow G. A project for ocular bioinformatics: NEIBank. Mol Vis 2002; 8:161-3.
29. Wistow G, Bernstein SL, Wyatt MK, Behal A, Touchman JW, Bouffard G, Smith D, Peterson K. Expressed sequence tag analysis of adult human lens for the NEIBank Project: over 2000 non-redundant transcripts, novel genes and splice variants. Mol Vis 2002; 8:171-84.
30. Wistow G, Bernstein SL, Ray S, Wyatt MK, Behal A, Touchman JW, Bouffard G, Smith D, Peterson K. Expressed sequence tag analysis of adult human iris for the NEIBank Project: steroid-response factors and similarities with retinal pigment epithelium. Mol Vis 2002; 8:185-95.
31. Chauhan BK, Reed NA, Zhang W, Duncan MK, Kilimann MW, Cvekl A. Identification of genes downstream of Pax6 in the mouse lens using cDNA microarrays. J Biol Chem 2002; 277:11539-48.
32. Wride MA, Mansergh FC, Adams S, Everitt R, Minnema SE, Rancourt DE, Evans MJ. Expression profiling and gene discovery in the mouse lens. Mol Vis 2003; 9:360-96.
33. Ahmed F, Torrado M, Zinovieva RD, Senatorov VV, Wistow G, Tomarev SI. Gene expression profile of the rat eye iridocorneal angle: NEIBank expressed sequence tag analysis. Invest Ophthalmol Vis Sci 2004; 45:3081-90.
34. Hawse JR, Hejtmancik JF, Huang Q, Sheets NL, Hosack DA, Lempicki RA, Horwitz J, Kantorow M. Identification and functional clustering of global gene expression differences between human age-related cataract and clear lenses. Mol Vis 2003; 9:515-37.
35. Dobbin K, Shih JH, Simon R. Statistical design of reverse dye microarrays. Bioinformatics 2003; 19:803-10.

The print version of this article was created on 8 May 2006. This reflects all typographical corrections and errata to the article through that date. Details of any changes may be found in the online version of the article.